Marine Chemistry 162 (2014) 10–18

Contents lists available at ScienceDirect

Marine Chemistry

journal homepage: www.elsevier.com/locate/marchem

A laboratory study of ikaite ($CaCO_3 \cdot 6H_2O$) precipitation as a function of pH, salinity, temperature and phosphate concentration

Yu-Bin Hu *, Dieter A. Wolf-Gladrow, Gerhard S. Dieckmann, Christoph Völker, Gernot Nehrke

Alfred-Wegener-Institut Helmholtz-Zentrum für Polar- und Meeresforschung (AWI), Postfach 12 01 61, D-27515 Bremerhaven, Germany

ARTICLE INFO

Article history:
Received 20 August 2013
Received in revised form 31 January 2014
Accepted 17 February 2014
Available online 27 February 2014

Keywords:
Ikaite
Calcium carbonate
Sea ice
Brine
Salinity
pH
Temperature
Phosphate

ABSTRACT

Ikaite ($CaCO_3 \cdot 6H_2O$) has only recently been discovered in sea ice, in a study that also provided first direct evidence of $CaCO_3$ precipitation in sea ice. However, little is as yet known about the impact of physico-chemical processes on ikaite precipitation in sea ice. Our study focused on how the changes in pH, salinity, temperature and phosphate (PO_4) concentration affect the precipitation of ikaite. Experiments were set up at pH from 8.5 to 10.0, salinities from 0 to 105 (in both artificial seawater (ASW) and NaCl medium), temperatures from 0 to −4 °C and PO_4 concentrations from 0 to 50 μmol kg^{-1}. The results show that in ASW, calcium carbonate was precipitated as ikaite under all conditions. In the NaCl medium, the precipitates were ikaite in the presence of PO_4 and vaterite in the absence of PO_4. The onset time (τ) at which ikaite precipitation started, decreased nonlinearly with increasing pH. In ASW, τ increased with salinity. In the NaCl medium, τ first increased with salinity up to salinity 70 and subsequently decreased with a further increase in salinity; it was longer in ASW than in the NaCl medium under the same salinity. τ did not vary with temperature or PO_4 concentration. These results indicate that ikaite is very probably the only phase of calcium carbonate formed in sea ice. PO_4 is not, as previously postulated, crucial for ikaite formation in sea ice. The change in pH and salinity is the controlling factor for ikaite precipitation in sea ice. Within the ranges investigated in this study, temperature and PO_4 concentration do not have a significant impact on ikaite precipitation.

1. Introduction

Ikaite ($CaCO_3 \cdot 6H_2O$) is a metastable phase of calcium carbonate, which normally forms in a cold environment and/or under high pressure (Marland, 1975). It is usually found in environments characterized by low temperatures (below 4 °C), high pH, high alkalinity, elevated concentrations of phosphate (PO_4) and organic matter (Buchardt et al., 1997; Rickaby et al., 2006). Although synthetic $CaCO_3 \cdot 6H_2O$ had already been known from laboratory studies in the nineteenth century (Pelouze, 1865), it was first found in nature at the bottom of the Ika Fjord in Greenland (Pauly, 1963) and later in deep-sea sediments (Suess et al., 1982). Recently, Dieckmann et al. (2008, 2010) discovered this mineral in sea ice, which at the same time, was the first direct evidence of $CaCO_3$ precipitation in natural sea ice. The occurrence of $CaCO_3$ is considered to play a significant role in the CO_2 flux of the sea ice system (Geilfus et al., 2012; Rysgaard et al., 2007).

At present it is not clear whether ikaite is the only calcium carbonate phase formed in sea ice (Dieckmann et al., 2010; Rysgaard et al., 2012). Calcium carbonate exists in six phases, namely, amorphous calcium carbonate (ACC), calcium carbonate monohydrate (MCC), calcium carbonate hexahydrate (ikaite) and three anhydrous phases: vaterite, aragonite and calcite. Ikaite is more soluble compared to the three anhydrous phases under normal atmospheric pressure (Bischoff et al., 1993). The precipitation of ikaite occurs only when the ion activity product (IAP) of Ca^{2+} and CO_3^{2-} in the solution exceeds the solubility product of ikaite ($K_{sp,\ ikaite}$). The activities of Ca^{2+} and CO_3^{2-} can be derived from their concentrations and activity coefficients. The values of the activity coefficient depend on solution ionic strength and temperature. In seawater at salinity 35 and temperature 25 °C, for example, the activity coefficients $\gamma_{Ca}^{2+} = 0.203$ and $\gamma_{CO_3}{}^{2-} = 0.039$ (Millero and Pierrot, 1998) are much smaller than 1. In normal seawater at a temperature above 0 °C, seawater is undersaturated with respect to ikaite (Bischoff et al., 1993). The precipitation of ikaite from seawater requires a higher concentration of Ca^{2+} and/or CO_3^{2-}, such as can be achieved in sea ice brine. Given the consideration that brine salinity can easily be over 200 at a corresponding temperature as low as −40 °C (Eicken, 2003), this extreme environment would greatly affect the chemical environment in brine with regard to calcium concentrations and dissolved inorganic carbon (DIC). Depending on the physico-chemical environments as well as biological effect (respiration and photosynthesis), brine pH can vary from less than 8 to up to 10 (Gleitz et al., 1995; Papadimitriou et al., 2007). Due to the inhibiting

* Corresponding author. Tel.: +49 471 4831 2001.
E-mail addresses: Yubin.Hu@awi.de (Y.-B. Hu), Dieter.Wolf-Gladrow@awi.de (D.A. Wolf-Gladrow), Gerhard.Dieckmann@awi.de (G.S. Dieckmann), Christoph.Voelker@awi.de (C. Völker), Gernot.Nehrke@awi.de (G. Nehrke).

http://dx.doi.org/10.1016/j.marchem.2014.02.003

role of PO_4 in the formation of anhydrous calcium carbonate polymorphs (Burton and Walter, 1990; Reddy, 1977), it is assumed that elevated PO_4 concentrations play a crucial role in ikaite formation (Buchardt et al., 1997; Dieckmann et al., 2010). However, this has never been tested under conditions representative for natural sea ice.

Despite of the apparent significance of calcium carbonate precipitation in sea ice, little is as yet known about the impact of physico-chemical processes on ikaite precipitation in sea ice. Papadimitriou et al. (2013) studied the solubility of ikaite in seawater-derived brines. In their study, the $K_{sp,\ ikaite}$ was measured in temperature–salinity coupled conditions, and based on simple modeling it was concluded that the precipitation of ikaite in sea ice possibly only occurs when brine pCO_2 is reduced. However, as the conditions leading to calcium carbonate precipitation in brine are normally coupled, a variation in sea ice temperature will change the brine salinity and also the chemical environment. It has therefore not been possible to distinguish/identify the dominant process that controls calcium carbonate precipitation under conditions representative for natural sea ice. In this study, we uncoupled the conditions in sea ice brine and each condition (pH, salinity, temperature and PO_4 concentration) was studied independently in the laboratory, in order to investigate whether ikaite was the only phase of calcium carbonate formed in sea ice and to qualify the effect of pH, salinity, temperature and PO_4 concentration on the precipitation of ikaite.

2. Methods

2.1. Preparation of stock solutions

Artificial seawater (ASW) of different salinities was prepared according to Millero (2006) with slight modifications. Ca^{2+} and HCO_3^- were not initially added in the ASW; the amount of $NaHCO_3$ and $CaCl_2$ was compensated for by adding NaCl. The amount of salt needed at salinity 70 and 105 was two and three times of that at salinity 35 (Table 1). Ten kilograms ASW of salinity 70 was prepared as a stock solution. In addition, 1 kg ASW of salinity 35 as well as salinity 105 was prepared separately. The salinity of the ASW stock solutions was checked with a conductivity meter (WTW Cond 330i). Subsamples of 10 mL stock solution of salinity 70 and 105 were diluted to salinity 35 before beginning with measurements; the differences between the theoretical and measured values were within ±0.2. Stock solutions of $CaCl_2$ and $NaHCO_3$ at concentrations of 2.5 mol kg^{-1} (soln) and 0.5 mol kg^{-1} (soln) were prepared by dissolving 183.775 g $CaCl_2 \cdot 2H_2O$ and 21.002 g $NaHCO_3$ into 500 g solutions using de-ionized water and subsequently stored in gas-tight Tedlar bags (SKC). All chemicals were obtained from Merck (EMSURE® ACS, ISO, Reag, Ph Eur) except $SrCl_2$ and H_3BO_3, which were from Carl Roth (p.a., ACS, ISO).

2.2. Experimental setup

Four parameters were studied: pH (8.5 to 10.0), salinities (0 to 105) both in ASW and the NaCl medium, temperatures (0 to −4 °C) and PO_4 concentrations (0 to 50 μmol kg^{-1}). The standard values were pH 9.0, salinity 70, temperature 0 °C, and PO_4 concentration 10 μmol kg^{-1} and only one of these quantities was varied at a time. Experiments were also carried out in the NaCl medium at salinities from 0 to 105 in the absence of PO_4 at pH 9 and temperature 0 °C.

In order to simulate the concentration processes of Ca^{2+} and DIC during sea ice formation, stock solutions of $CaCl_2$ and $NaHCO_3$ (Ca^{2+}: DIC = 5:1, which is the typical concentration ratio in seawater) were pumped from the Tedlar bags into a Teflon reactor vessel with 250 g working solution using a high precision peristaltic pump (IPC-N, Ismatec) at a constant pumping rate of 20 μL min^{-1} (Fig. 1). The solution was stirred at 400 rpm and the temperature was controlled by water-bath using double walled water jackets. pH electrodes (Metrohm 6.0253.100) were calibrated using NBS buffers 7.000 ± 0.010 and 10.012 ± 0.010 (Radiometer analytical, IUPAC standard). The pH of the solution was kept constant by adding 0.5 mol L^{-1} NaOH which was controlled by a titration system (TA20 plus, SI Analytics). pH and the volume of NaOH added to the solution were recorded every 10 s. Depending on the experimental conditions, the maximum input of $CaCl_2$, $NaHCO_3$ and NaOH into the working solution during the experiments is within a few mL, which did not have a significant effect on solution salinity. Duplicates for each experimental condition were run in parallel.

2.3. Onset time determination

We use the timespan between the start of the titration and the onset of ikaite precipitation, called "onset time (τ)", for the analysis of different experiments. This onset time includes the time for the solution to reach saturation ($\Omega = 1$) with respect to ikaite and the time between reaching the $\Omega = 1$ level and the onset of precipitation (usually at a much higher Ω value). Therefore, τ should be controlled by both thermodynamic and kinetic effects.

While ikaite is precipitated from the solution, CO_2 is released, which leads to a decrease in solution pH. This rapid change in pH could have been used to ascertain the onset of precipitation. However, during the experiment, pH in the solution was kept constant by the addition of NaOH. Therefore, the change in NaOH volume added into the reactor vessel was used to determine τ as indicated in Fig. 2. In order to obtain a higher accuracy, τ was determined from the deviation of NaOH volume change (ΔV) relative to the time interval ($\Delta t = 2$ min). The point where the slope $\Delta V/\Delta t$ started to increase was considered as the onset of ikaite precipitation.

2.4. Crystal identification

Immediately after the crystals were precipitated, indicated by the change in the volume of NaOH addition (Section 2.3), around 2 mL of the well-stirred solution was sampled together with the crystals by means of a pipette and quickly transferred to a glass petri dish. The morphology of the crystals was characterized using a microscope (Zeiss, Axiovert 200M) with an objective of 63× magnification. The phase identification of the crystals was done by means of Raman microscopy. This method can be used to reliably distinguish between the various polymorphs of calcium carbonate (Nehrke et al., 2012; Tlili et al., 2001). The confocal Raman microscope (WITec®, Ulm, Germany) was equipped with a diode laser (532 nm) and an Olympus® 20× Teflon coated water submersible objective. During the Raman measurements, crystals were maintained in the original solution and placed in a glass petri dish, which was kept cold using an ice-water bath.

2.5. Evolution of the ion activity product of calcium and carbonate

The evolution of the IAP of Ca^{2+} and CO_3^{2-} in the solution under different experimental conditions was calculated by using the chemical equilibrium model Visual-Minteq 3.0 (Gustafsson, 2011) modified by

Table 1
The compounds of ASW at different salinities.

Amount of salt (g) needed in 1000 g solution			
Salt	S = 35	S = 70	S = 105
NaCl	25.122	50.245	75.368
$MgCl_2 \cdot 6H_2O$	10.738	21.477	32.215
Na_2SO_4	4.010	8.020	12.030
KCl	0.699	1.398	2.097
$SrCl_2 \cdot 6H_2O$	0.024	0.048	0.072
KBr	0.100	0.200	0.300
H_3BO_3	0.025	0.051	0.076
$NaHCO_3$	–	–	–
$CaCl_2 \cdot 2H_2O$	–	–	–

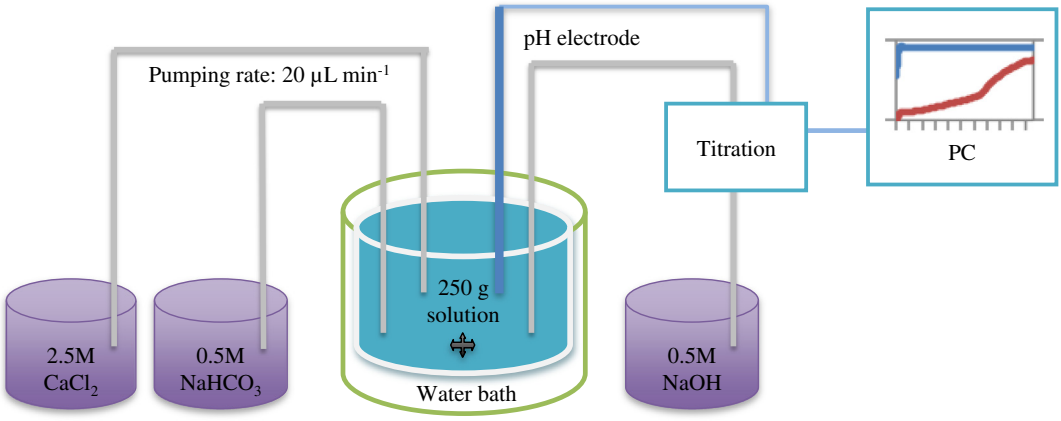

Fig. 1. Experimental setup for calcium carbonate precipitation under varied experimental conditions.

the implementation of $K_{sp,\ ikaite}$ according to Bischoff et al. (1993). The solubility constant of ikaite ($K_{sp,\ ikaite}$) was derived from log $K_{sp,\ ikaite} = 0.15981 - 2011.1 / T$, where T = K (Bischoff et al., 1993). Since most equilibrium constants (including $K_{sp,\ ikaite}$) at high salinities and low temperatures are not well known, extrapolations of functional relationships had to be used. The input parameters for each run were the same as used in the experiments, and the model was run in the function of "titration", simulating the experimental pumping of $CaCl_2$ and $NaHCO_3$ into the working solution. As in most models, the calculation of ionic activities is not very accurate at high salinities, especially the calculation of CO_3^{2-} activity, the evolution trends under different experimental conditions will be discussed in this study instead of referring to the absolute values.

2.6. CO_2 system calculation

The fraction of CO_3^{2-} in DIC (CO_3^{2-} fraction, for short) under all the experimental conditions was calculated from pH and DIC by using CO2SYS (Pierrot et al., 2006). The results of CO2SYS are not reliable for the calculation of the CO_2 system at high salinities because the functional expressions for the equilibrium constants are based on measurements over a limited range of salinities and temperatures. Here, we chose two sets of carbonate equilibrium constants, one from Mehrbach et al. (1973) as refitted by Dickson and Millero (1987) (referred to as constants_a), and the other one from Millero (2010) (referred to as constants_b), to evaluate the sensitivity of the calculated CO_3^{2-} fraction to uncertainties in the magnitude of the equilibrium constants. The remaining parameters were the same: $K_{HSO_4^-}$ was from Dickson (1990); $[B]_T$ value was from Uppström (1974) and the pH_{NBS} scale was applied. The input parameters for the CO_2 system calculation were consistent with the experimental conditions except that the DIC was fixed at 2000 μmol kg^{-1} for each run, since the change in DIC concentration does not affect the CO_3^{2-} fraction calculation.

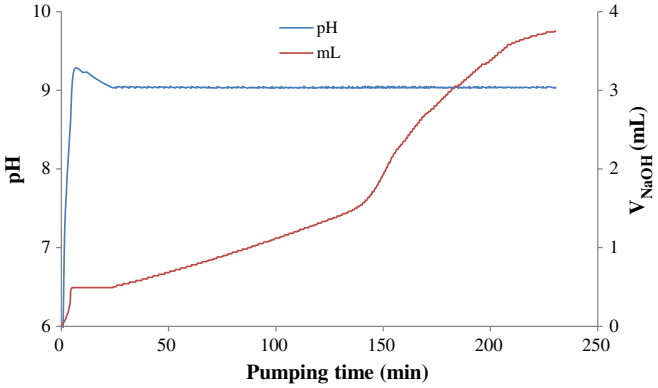

Fig. 2. An illustration of a typical NaOH titration profile obtained at pH 9, salinity (ASW) 70, temperature 0 °C and phosphate concentration 10 μmol kg^{-1}.

3. Results

3.1. Effect of experimental conditions on the calcium carbonate polymorph precipitated

According to the vibration ν_1 and ν_4 of CO_3^{2-}, two types of Raman spectra were distinguished in this study. After a comparison with the available references (Behrens et al., 1995; Tlili et al., 2001), ikaite was identified by the vibrational modes ν_1 (1071 cm^{-1}) and ν_4 (718 cm^{-1}), and vaterite was identified by the two doublets of the vibration modes ν_1 (1075 cm^{-1}, 1090 cm^{-1}) and ν_4 (742 cm^{-1}, 752 cm^{-1}).

In ASW, according to the Raman measurements (Fig. 3a), ikaite is the only calcium carbonate polymorph precipitated at pH ranging from 8.5 to 10.0, salinities from 0 to 105, temperatures from 0 to −4 °C and PO_4 concentrations from 0 to 50 μmol kg^{-1}. The morphology of ikaite crystals precipitated from ASW is similar under all the conditions, with an average crystal size of approximately 20 μm (Fig. 3b). The morphology resembles that of natural ikaite crystals found in sea ice (Rysgaard et al., 2013), however, crystals in our study are generally smaller.

In the NaCl medium, and the presence of 10 μmol kg^{-1} PO_4, according to the Raman measurements (Fig. 3c), ikaite is the only precipitate in the salinity range from 0 to 105. The crystal size is similar to the one observed for the crystals precipitated from ASW. However, the morphology of ikaite crystals differs (Fig. 3d). In the absence of PO_4 and the same salinity range, vaterite (see Raman spectrum given in Fig. 3e) is the dominant calcium carbonate polymorph precipitated and only few ikaite crystals were observed. The small spherical crystals shown in Fig. 3f are vaterite with an average size of ~2 μm (within the same size range as described by Nehrke and Van Cappellen (2006)) whereas the large crystal in the middle of Fig. 3f is ikaite.

3.2. Onset time of ikaite under different experimental conditions

Onset time (τ) under different pH, salinities (both in ASW and NaCl medium), temperatures and PO_4 concentrations is illustrated in Fig. 4(a–d) and Table 2. At pH from 8.5 to 10.0, τ decreases nonlinearly with increasing pH; it decreases steeply at low pH and then slows down at high pH. At salinities from 0 to 105, in ASW, τ increases with salinity; in the NaCl medium, τ first increases with salinity and above salinity 70, it decreases slightly. τ is longer in ASW than in the NaCl medium under the same salinity conditions. There is no significant difference in τ in the

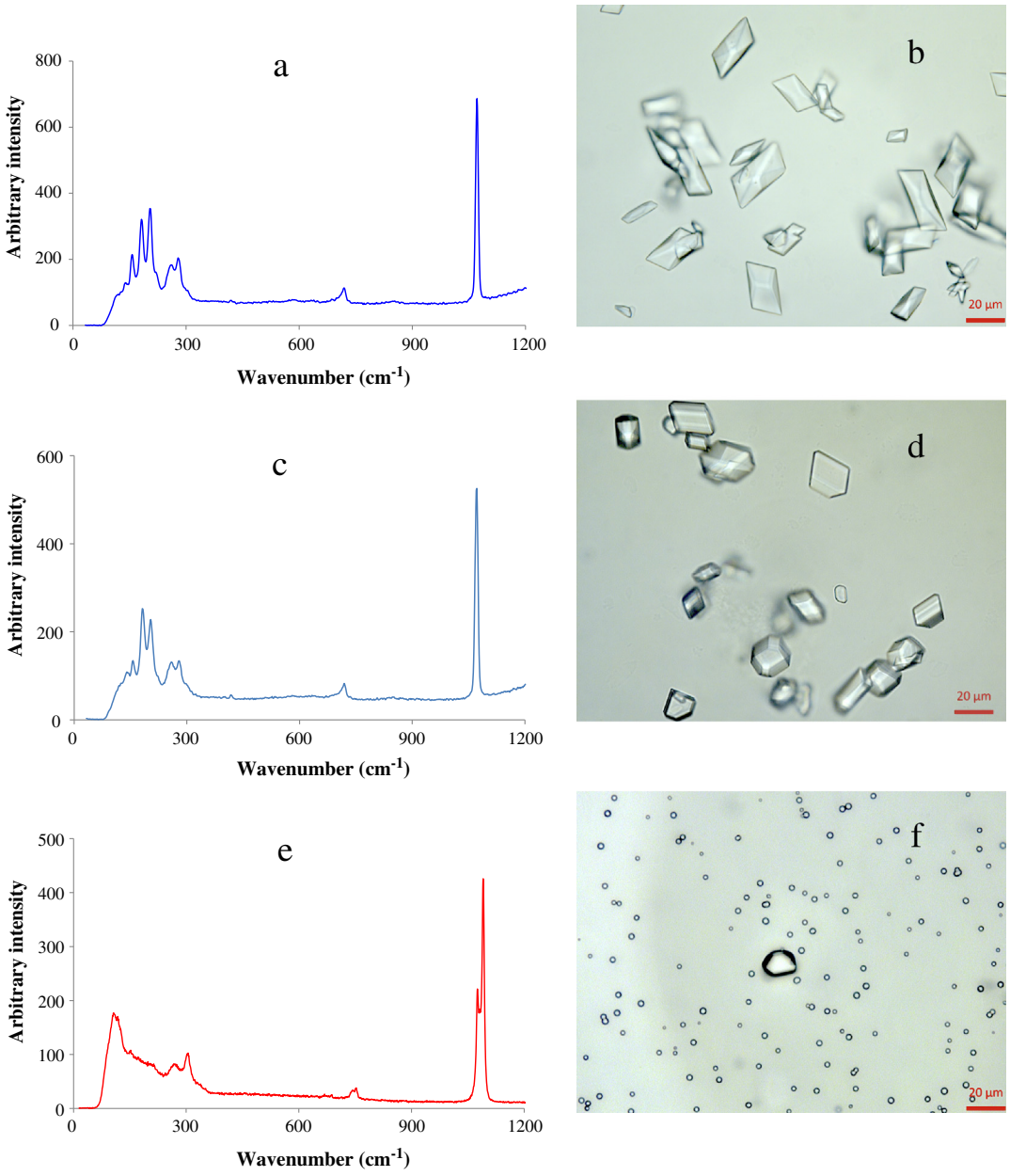

Fig. 3. Ikaite Raman spectrum (a) and morphology (b) obtained at the experimental condition pH 9.0, salinity (ASW) 70, temperature 0 °C, phosphate concentration 10 μmol kg^{-1}, and representative for all precipitates in the ASW medium. Ikaite Raman spectrum (c) and morphology (d) obtained at the experimental condition pH 9.0, salinity (NaCl medium) 70, temperature 0 °C, phosphate concentration 10 μmol kg^{-1}, and representative for all precipitates in the NaCl medium in the presence of PO_4. Vaterite Raman spectrum (e) and morphology (f) obtained at the experimental condition pH 9.0, salinity (NaCl medium) 105, temperature 0 °C, phosphate concentration 0 μmol kg^{-1}, and representative for all precipitates in the NaCl medium in the absence of PO_4.

temperature range from 0 to −4 °C and in the PO_4 concentration range from 0 to 50 μmol kg^{-1}.

3.3. Evolution of the ion activity product of Ca^{2+} and CO_3^{2-}

The evolution of the common logarithmic ion activity product of Ca^{2+} and CO_3^{2-} (log (IAP)) until the onset of ikaite precipitation and the solution supersaturation at the onset of ikaite precipitation (Ω = IAP / $K_{sp,\ ikaite}$) under different pH, salinities (both in ASW and NaCl medium), temperatures and PO_4 concentrations are illustrated in Fig. 5(a–e) and Table 2. At pH from 8.5 to 10.0, the rates of log (IAP) evolution are much faster at higher pH but the evolution curves are getting closer with the increase in pH. Ω increases with increasing pH. At salinity from 0 to 105, log (IAP) evolution shows a similar pattern in ASW and NaCl medium: that is at salinity 0, the evolution is much faster than those at salinities equal or larger than 35. And the evolution curves are getting closer with the increase in salinity. The rates in log (IAP) evolution are slower in ASW than those in the NaCl medium under the same salinity conditions. For example, at salinity 70, the time to reach ikaite solubility (t_s) is 72 min in ASW while it is 65 min in the NaCl medium (Table 2). Ω is similar in ASW in this studied salinity range; while it decreases with increasing salinity in the NaCl medium. At temperatures from 0 to −4 °C, the curves of log (IAP) evolution overlap as do the curves of log (IAP) evolution at PO_4 concentrations from 0 to 50 μmol kg^{-1}. There is no significant difference in Ω in this temperature and PO_4 concentration range.

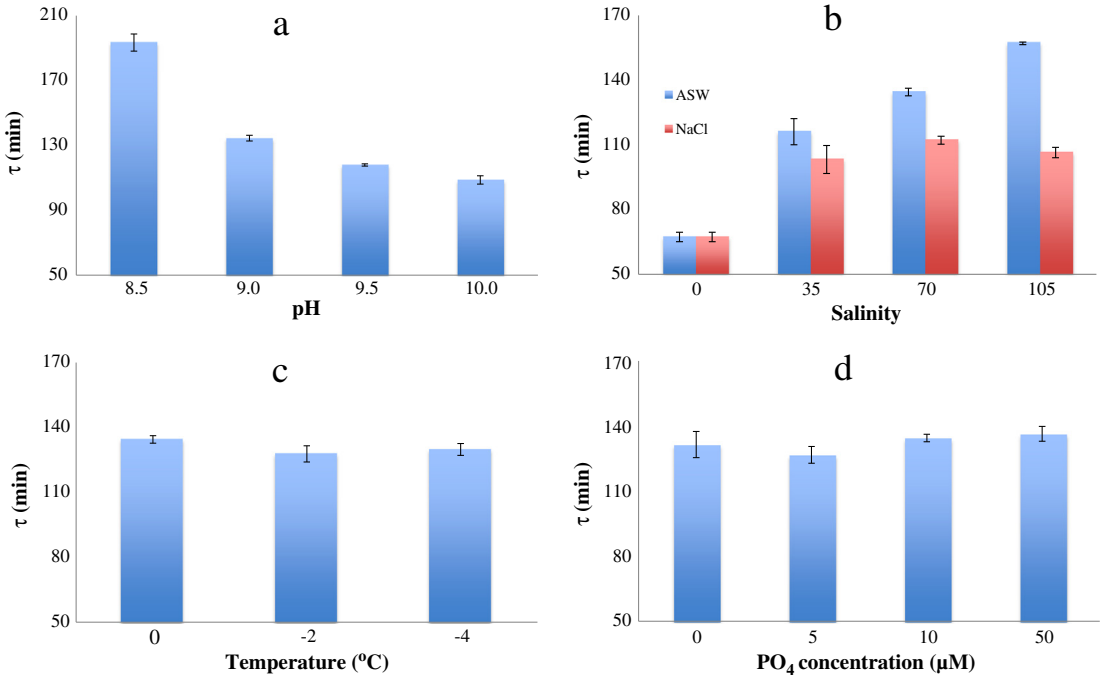

Fig. 4. Changes in τ with pH (a), salinity (b), temperature (c) and phosphate concentration (d).

4. Discussion

4.1. Ikaite crystal size

The smaller size of ikaite crystals in our experiments compared to those found in natural sea ice might be due to the much faster precipitation rate under laboratory conditions, which favors calcium carbonate nucleation over further growth of crystals (Vekilov, 2010). In sea ice, the precipitation of ikaite probably goes through a much slower process, allowing the crystals to grow larger. However, the size of natural ikaite in sea ice could also be limited by the dimensions of the brine pockets or brine channels (Dieckmann et al., 2008).

4.2. Effect of PO_4 on the polymorph of calcium carbonate precipitated

The different precipitates in the NaCl medium with and without PO_4 indicate that the presence of PO_4 is important for ikaite formation in the NaCl medium. This result is consistent with other studies stating that ikaite is usually found in an elevated PO_4 environment (Buchardt et al., 1997; Council and Bennett, 1993).

The different precipitates in ASW and the NaCl medium in the absence of PO_4 indicate that PO_4 is not crucial for ikaite formation in ASW. It has been reported (Bischoff et al., 1993; Fernández-Díaz et al., 2010) that Mg^{2+} and SO_4^{2-} ions in seawater could also inhibit the formation of more stable phases of calcium carbonate, and thus could

Table 2
Pumping time until the solution reaching ikaite solubility (t_s), onset time (τ) and the common logarithmic ion activity product of calcium and carbonate (log (IAP)) and solution supersaturation ($\Omega = IAP / K_{sp,\ ikaite}$) at the onset of ikaite precipitation under different pH, salinity (ASW and NaCl medium), temperature and phosphate concentration conditions. The standard deviation of τ and log (IAP) is derived from duplicate experiments.

Exp. conditions	Exp. variations	t_s (min)	τ min	Log (IAP)	Ω
pH effect: at S (ASW) 70, T 0 °C, PO_4 10 μM	8.5	112	193 ± 5.3	−6.73 ± 0.025	3.02
	9.0	72	134 ± 1.8	−6.67 ± 0.011	3.47
	9.5	54	118 ± 0.7	−6.53 ± 0.005	4.68
	10.0	46	109 ± 2.6	−6.48 ± 0.020	5.37
S (AWI) effect: at pH 9.0, T 0 °C, PO_4 10 μM	0	28	67 ± 2.2	−6.59 ± 0.021	4.17
	35	62	116 ± 6.1	−6.68 ± 0.051	3.47
	70	72	134 ± 1.8	−6.67 ± 0.011	3.47
	105	78	157 ± 0.6	−6.61 ± 0.003	3.98
S (NaCl) effect: at pH 9.0, T 0 °C, PO_4 10 μM	0	28	67 ± 2.2	−6.59 ± 0.021	4.17
	35	58	103 ± 6.5	−6.72 ± 0.049	3.09
	70	65	112 ± 1.8	−6.74 ± 0.014	2.95
	105	70	106 ± 2.4	−6.84 ± 0.019	2.29
T effect: at pH 9.0, S (ASW) 70, PO_4 10 μM	0 °C	72	134 ± 1.8	−6.67 ± 0.011	3.47
	−2 °C	69	128 ± 3.7	−6.73 ± 0.023	3.39
	−4 °C	66	130 ± 2.7	−6.74 ± 0.017	3.72
	−10 °C	60	NA	NA	NA
PO_4 concentration effect: at pH 9.0, S (ASW) 70, T 0 °C	0 μM	72	131 ± 6.0	−6.69 ± 0.037	3.31
	5 μM	72	127 ± 3.9	−6.71 ± 0.024	3.16
	10 μM	72	134 ± 1.8	−6.67 ± 0.011	3.47
	50 μM	72	136 ± 3.4	−6.66 ± 0.022	3.55

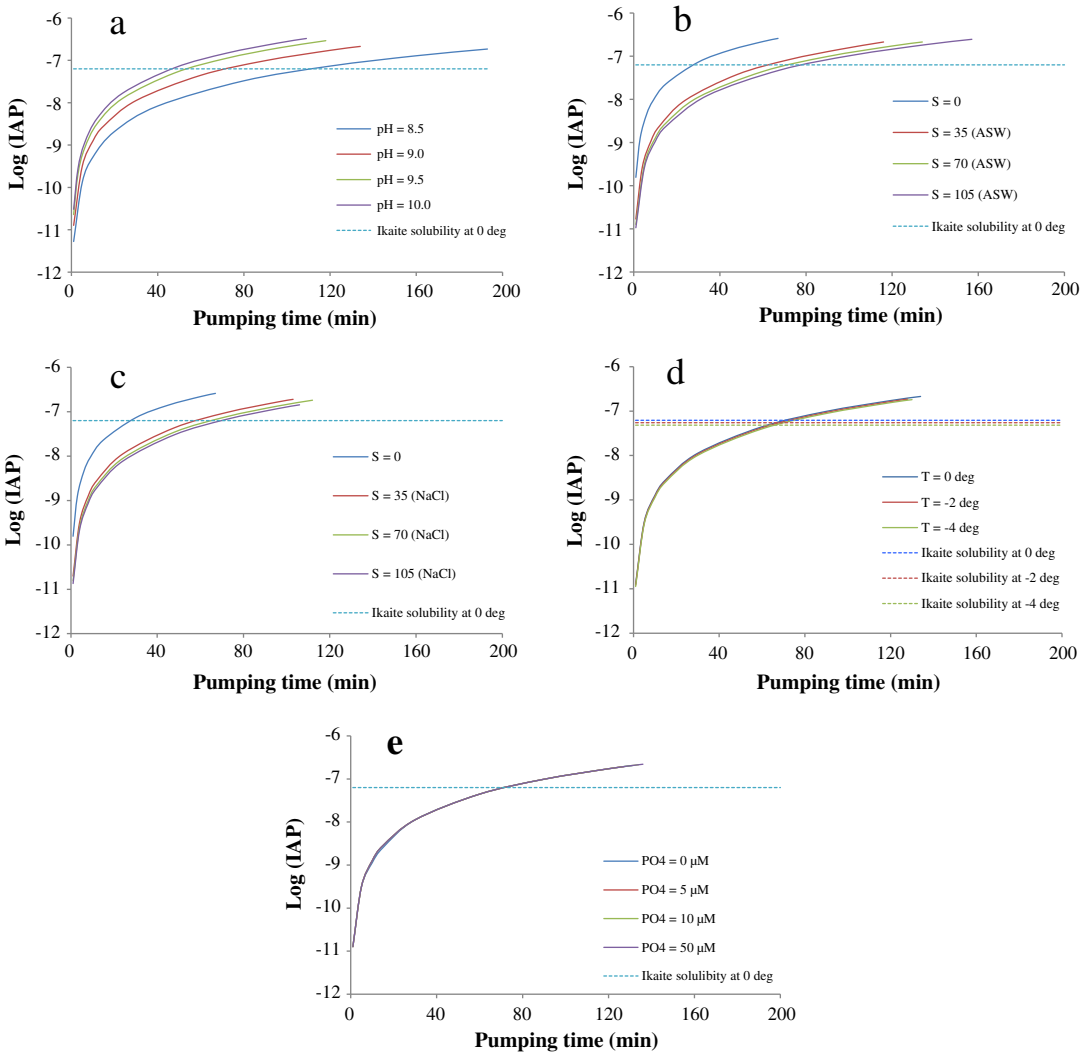

Fig. 5. Evolution of log (IAP) at different pH levels (a), salinities in ASW (b), salinities in the NaCl medium (c), temperatures (d) and phosphate concentrations (e).

favor ikaite formation. This might explain why ikaite was also found in sea ice even at very low PO_4 concentrations (Dieckmann et al., 2010).

4.3. Effect of experimental conditions on ikaite precipitation

According to the evolution curves of log (IAP) under all the experimental conditions, we can conclude that τ is mainly controlled by the rates of log (IAP) evolution and also greatly affected by the kinetic effect, such as inhibitor ions. In the following sub-sections, the effect of experimental conditions on ikaite precipitation will focus on the factors controlling the rates of log (IAP) evolution as well as the kinetic effect.

4.3.1. pH effect

In ASW at a constant salinity of 70 and temperature of 0 °C, the activity coefficients of both Ca^{2+} and CO_3^{2-} do not change. Therefore, we only need to focus on the change in CO_3^{2-} concentration with variations of pH. According to the calculation results from CO2SYS, under the same conditions, the results obtained by using constants_a and constants_b show a similar trend (Fig. 6a). The increase in pH can greatly increase the CO_3^{2-} fraction in this studied pH range, resulting in a much faster approach to ikaite solubility (Fig. 5a). However, the decrease in τ with pH is not linear, which is much faster at low pH than at high pH. This is because the CO_3^{2-} fraction cannot increase infinitely; the increase in the CO_3^{2-} fraction will slow down at high pH and the CO_3^{2-} fraction will approach 1. We can speculate that above a certain pH (depending on the salinity and temperature conditions, since the CO_3^{2-} fraction is also affected by them, as is discussed in Sections 4.3.2 and 4.3.3), the increase in pH will not have an impact on the CO_3^{2-} fraction, and therefore has no effect on ikaite precipitation. We notice that Ω in this studied pH range increases from 3.02 to 5.37 with increasing pH (Table 2). This indicates that if the evolution of log (IAP) is slow, ikaite could be precipitated at a much lower supersaturation level. This is also confirmed by a second study, which shows that at different pumping rates of Ca^{2+} and DIC, Ω is low at slow pumping rates (Hu et al., submitted).

4.3.2. Salinity effect

The different trends in τ in ASW and the NaCl medium indicate that the effect of salinity on ikaite precipitation is not straightforward. First, according to the calculation results from CO2SYS, although there is large uncertainty in predicting the exact CO_3^{2-} fraction change with salinity at high salinities, both the results obtained from two sets of constants show a similar trend (Fig. 6b): the CO_3^{2-} fraction increases with salinity (referred to as a positive effect). However, the increase in salinity implies an increase in ionic strength as well and thus a reduction in the activities of both Ca^{2+} and CO_3^{2-} (referred to as a negative effect). This negative effect is much stronger in ASW than in the NaCl medium, since there are ion species like SO_4^{2-} and Mg^{2+} in ASW, which could strongly form ion pairs with Ca^{2+} and

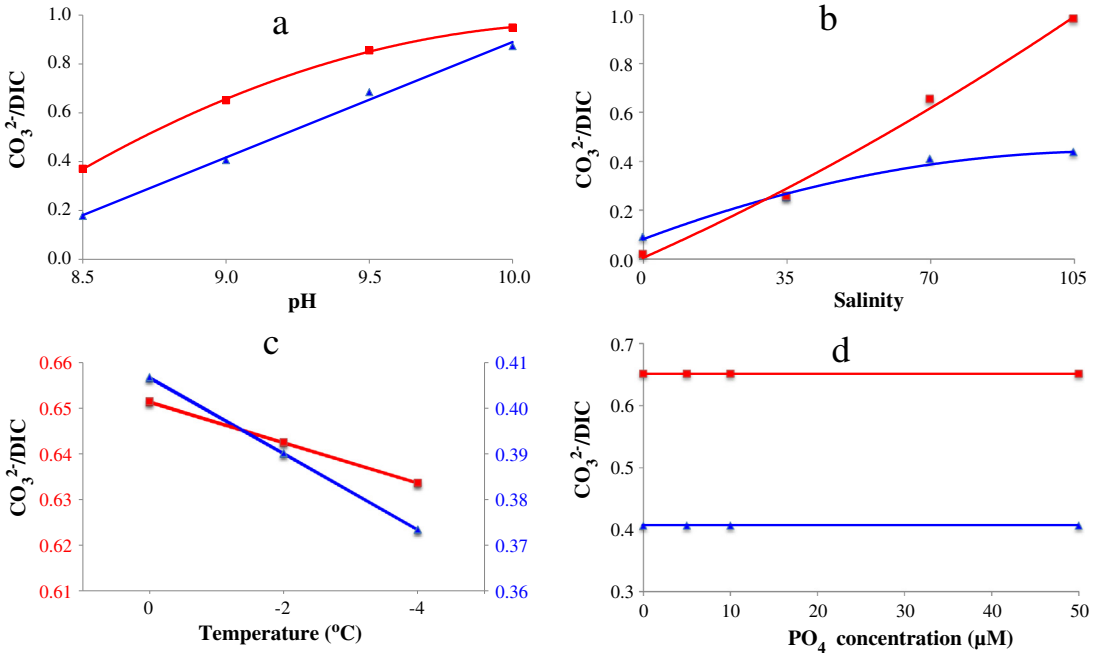

Fig. 6. CO_3^{2-} fraction relative to pH (a), salinity (b), temperature (c) and phosphate concentration (d) based on two sets of constants (constants_a, in blue triangle; constants_b, in red square). (For interpretation of the references to color in this figure legend, the reader is referred to the web version of this article.)

CO_3^{2-} (Kester and Pytkowicz, 1969; Pytkowicz and Hawley, 1974), and thus further reduce the activities of Ca^{2+} and CO_3^{2-}. This explains the slower evolution of log (IAP) in ASW than in the NaCl medium under the same salinity conditions.

In ASW or NaCl medium, the rates in log (IAP) evolution are slower at higher salinities but the evolution curves of log (IAP) from salinity 35 to 105 are getting closer (Fig. 5b & 5c), indicating that the negative effect slightly overweighs the positive one, but that the differences between them become smaller with increasing salinity. However, τ decreases slightly above salinity 70 in NaCl medium. According to a study of calcite crystallization by Bischoff (1968), the calcite nucleation rate was found to be proportional to the square root of solution ionic strength. Thus, we speculate that the increase in salinity (ionic strength) might also accelerate ikaite nucleation rate, which explains the decrease in Ω with increasing salinity in the NaCl medium. Nevertheless, the large increase in τ in ASW in the same salinity range requires another explanation. It was shown by other studies (Reddy and Wang, 1980; Zhang and Dawe, 2000) that Mg^{2+} can strongly retard calcium carbonate precipitation. Therefore, we might speculate that the longer τ at higher salinities in ASW is due to the presence of Mg^{2+}; the inhibiting effect becomes stronger with increasing Mg^{2+} concentration and this effect overweighs the ionic strength catalysis in ASW.

4.3.3. Temperature effect

The similar τ at temperatures from 0 to −4 °C indicates that the change in temperature does not have a significant impact on ikaite precipitation in this studied temperature range. According to the calculation results from CO2SYS, although the absolute values of the change in the CO_3^{2-} fraction with pH from two sets of constants are quite different, the trend is similar (Fig. 6c): the decrease in temperature only slightly reduces the CO_3^{2-} fraction, which explains the overlapping of log (IAP) evolution curves in Fig. 5d. On the other hand, log $K_{sp,\ ikaite}$ decreases by 0.11 from temperature 0 to −4 °C (Fig. 5d), indicating that lower temperatures would favor the precipitation of ikaite. However, no clear trend of temperature effect on ikaite precipitation can be concluded from this narrow studied temperature range.

Unfortunately, based on the relationship between salinity and temperature in sea ice (Feistel, 2008), the freezing temperature of brine is −4.03 °C at salinity 70, which limited the range of temperature investigated in this study. Nevertheless, according to the trend in the time required to reach ikaite solubility (t_s) in Table 2, we see a steady decrease in t_s with decreasing temperature as low as −10 °C as predicted by the model calculations. Thus, from a thermodynamic point of view, we could infer that lower temperatures might have slightly positive influence on ikaite precipitation. However, we cannot exclude the kinetic effect that might arise from lower temperatures and thus the overall effect of temperature on ikaite precipitation at lower temperatures (<−4 °C) remains unknown.

4.3.4. PO_4 effect

The similar τ at PO_4 concentrations from 0 to 50 μmol kg^{-1} indicates that the change in PO_4 concentration does not have an impact on ikaite precipitation in this studied PO_4 concentration range. According to the calculation results from CO2SYS, although the CO_3^{2-} fraction obtained from two different sets of constants largely differs, both show a similar trend (Fig. 6d): the CO_3^{2-} fraction is not affected by PO_4 concentrations. On the other hand, the concentrations of PO_4 investigated in this study even as high as 50 μmol kg^{-1} are much lower compared to the bulk solution indicating that the change in PO_4 concentration has no impact on the solution ionic strength at salinity 70. So the change in PO_4 concentration barely affects the activities of Ca^{2+} and CO_3^{2-}. From a thermodynamic point of view, the change in PO_4 concentration on the solution ionic strength, activities of Ca^{2+} and CO_3^{2-} and thus on IAP evolution is negligible. This explains the overlapping of log (IAP) curves in this studied PO_4 concentration range. However, besides the thermodynamic effect, kinetics due to the inhibiting effect of PO_4 is also considered to play an important role in calcium carbonate precipitation. It was shown in other studies (Morse et al., 2007; Reddy, 1977) that PO_4 could strongly retard the precipitation of calcite and aragonite in the solution. According to our results on Ω (Table 2), which shows no difference in the studied PO_4 concentration range, it appears that PO_4 does

not have any kinetic effect on ikaite precipitation either, which is consistent with the study of Bischoff et al. (1993).

4.4. Application to natural sea ice scenario

In natural sea ice, temperature is the driving force for the physico-chemical processes in sea ice brine. With the decrease in brine temperature, brine salinity as well as the concentrations of Ca^{2+} and DIC increases correspondingly. However, the change in temperature might not have a significant direct impact on ikaite precipitation. Ikaite precipitation in natural sea ice is mainly controlled by the brine concentration rate, pH and salinity (ionic strength and the concentration of inhibitor ions).

Ikaite precipitation in natural sea ice is mainly found in the upper layer, and the concentration of ikaite decreases with sea ice depth (Dieckmann et al., 2008; Fischer et al., 2013). This might be due to the high concentrations of Ca^{2+} and DIC resulting from high concentration rates of brine solutions in the upper layer of the cold sea ice, even though low pH and high salinities in this layer are not the favored conditions.

Recently, high concentrations of ikaite were found in both the top and bottom of sea ice with a minimum in the middle section of sea ice (Geilfus et al., 2013). The reason for the high ikaite concentrations on the top of sea ice should be the same as in the first case; the increase in ikaite concentration in the bottom of sea ice is probably caused by the increase in pH due to the photosynthetic activity. Brine pH has been reported to be as high as 10 in sea ice (Gleitz et al., 1995). As a result, although the brine concentration in the bottom of sea ice is low due to the warm sea ice, the dramatic increase in brine pH due to the photosynthetic activity would greatly increase the CO_3^{2-} fraction thus enhancing the likelihood of ikaite precipitation in sea ice, even though the concentrations of Ca^{2+} and DIC are low due to relatively warmer sea ice.

It is important to point out that in our experimental design, the solution pH was kept constant during the course of experiment. However, in natural sea ice, the precipitation of ikaite will lead to a decrease in pH, resulting in a decrease in solution supersaturation. As a consequence, the equilibrium between the solid phase and liquid phase could be established in a short time and thus the precipitation will cease until the equilibrium is broken again by further concentration of brine solution and/or pH change.

5. Conclusions

The effect of physico-chemical processes in sea ice on calcium carbonate precipitation was investigated. Ikaite ($CaCO_3 \cdot 6H_2O$) is the only polymorph of calcium carbonate precipitated under all studied experimental conditions in artificial seawater (ASW), suggesting that ikaite is very likely the only polymorph of calcium carbonate formed in natural sea ice as well. PO_4 is crucial for ikaite formation in the NaCl medium. However, it is not important for ikaite formation under ASW conditions. pH is the controlling factor in ikaite precipitation due to its strong impact on CO_3^{2-} concentrations. Ionic strength has two opposite thermodynamic effects on ikaite precipitation, as the change in solution ionic strength affects the CO_3^{2-} concentrations and the activities of Ca^{2+} and CO_3^{2-} in opposite directions. The increase in ionic strength could also kinetically accelerate the ikaite nucleation rate. In ASW, the presence of inhibitor ions could strongly retard ikaite precipitation. The large variations in PO_4 concentrations have no impact on ikaite precipitation, indicating that ikaite precipitation is neither thermodynamically nor kinetically affected by PO_4.

Acknowledgments

Gernot Nehrke is supported by the DFG by grant NE 1564/1-1 (SPP 1158). Yu-Bin Hu is the beneficiary of a doctoral grant from the AXA Research Fund.

References

Behrens, G., Kuhn, L.T., Ubic, R., Heuer, A.H., 1995. Raman spectra of vateritic calcium carbonate. Spectrosc. Lett. 28 (6), 983–995.
Bischoff, J.L., 1968. Kinetics of calcite nucleation: magnesium ion inhibition and ionic strength catalysis. J. Geophys. Res. 73 (10), 3315–3322.
Bischoff, J.L., Fitzpatrick, J.A., Rosenbauer, R.J., 1993. The solubility and stabilization of ikaite ($CaCO_3 \cdot 6H_2O$) from 0° to 25 °C: environmental and paleoclimatic implications for thinolite tufa. J. Geol. 101 (1), 21–33.
Buchardt, B., et al., 1997. Submarine columns of ikaite tufa. Nature 390, 129–130.
Burton, E.A., Walter, L.M., 1990. The role of pH in phosphate inhibition of calcite and aragonite precipitation rates in seawater. Geochim. Cosmochim. Acta 54 (3), 797–808.
Council, T.C., Bennett, P.C., 1993. Geochemistry of ikaite formation at Mono Lake, California: implications for the origin of tufa mounds. Geology 21 (11), 971–974.
Dickson, A.G., 1990. Standard potential of the reaction: $AgCl(s) + 1/2\ H_2(g) = Ag(s) + HCl(aq)$, and the standard acidity constant of the ion HSO_4^- in synthetic sea water from 273.15 to 318.15 K. J. Chem. Thermodyn. 22 (2), 113–127.
Dickson, A.G., Millero, F.J., 1987. A comparison of the equilibrium constants for the dissociation of carbonic acid in seawater media. Deep-Sea Res. 34 (10), 1733–1743.
Dieckmann, G.S., et al., 2008. Calcium carbonate as ikaite crystals in Antarctic sea ice. Geophys. Res. Lett. 35 (8), L08501.
Dieckmann, G.S., et al., 2010. Brief communication: ikaite ($CaCO_3 \cdot 6H_2O$) discovered in Arctic sea ice. Cryosphere 4 (2), 227–230.
Eicken, H., 2003. From the microscopic, to the macroscopic, to the regional scale: growth, microstructure and properties of sea ice. In: Thomas, D.N., Dieckmann, G.S. (Eds.), Sea Ice: An Introduction to Its Physics, Chemistry, Biology and Geology. Blackwell Science, Oxford, pp. 22–81.
Feistel, R., 2008. A Gibbs function for seawater thermodynamics for −6 to 80 °C and salinity up to 120 g kg^{-1}. Deep-Sea Res. I Oceanogr. Res. Pap. 55 (12), 1639–1671.
Fernández-Díaz, L., Fernández-González, Á., Prieto, M., 2010. The role of sulfate groups in controlling $CaCO_3$ polymorphism. Geochim. Cosmochim. Acta 74 (21), 6064–6076.
Fischer, M., et al., 2013. Quantification of ikaite in Antarctic sea ice. Antarct. Sci. 25 (03), 421–432.
Geilfus, N.X., et al., 2012. Dynamics of pCO_2 and related air–ice CO_2 fluxes in the Arctic coastal zone (Amundsen Gulf, Beaufort Sea). J. Geophys. Res. 117, C00G10.
Geilfus, N.X., et al., 2013. First estimates of the contribution of $CaCO_3$ precipitation to the release of CO_2 to the atmosphere during young sea ice growth. J. Geophys. Res. 118 (1), 244–255.
Gleitz, M., Loeff, M.R.v.d, Thomas, D.N., Dieckmann, G.S., Millero, F.J., 1995. Comparison of summer and winter inorganic carbon, oxygen and nutrient concentrations in Antarctic sea ice brine. Mar. Chem. 51 (2), 81–91.
Gustafsson, J.P., 2011. Visual MINTEQ ver. 3.0. KTH. Department of Land and Water Resources Engineering, Stockholm, Sweden (http://www2.lwr.kth.se/English/OurSoftware/vminteq/).
Hu, Y.-B., Wolthers, M., Nehrke, G., 2014. Is amorphous calcium carbonate (ACC) a necessary precursor for ikaite ($CaCO_3 \cdot 6H_2O$) formation? (submitted to Crystal Research and Technology).
Kester, D.R., Pytkowicz, R.M., 1969. Sodium, magnesium, and calcium sulfate ion-pairs in seawater at 25 °C. Limnol. Oceanogr. 14 (5), 686–692.
Marland, G., 1975. The stability of $CaCO_3 \cdot 6H_2O$ (ikaite). Geochim. Cosmochim. Acta 39, 83–91.
Mehrbach, C., Culberson, C.H., Hawley, J.E., Pytkowicz, R.M., 1973. Measurement of the apparent dissociation constants of carbonic acid in seawater at atmospheric pressure. Limnol. Oceanogr. 18 (6), 897–907.
Millero, F.J., 2006. Chemical Oceanography, 3rd ed. CRC Press, Boca Raton, FL.
Millero, F.J., 2010. Carbonate constants for estuarine waters. Mar. Freshw. Res. 61 (2), 139–142.
Millero, F., Pierrot, D., 1998. A chemical equilibrium model for natural waters. Aquat. Geochem. 4 (1), 153–199.
Morse, J.W., Arvidson, R.S., Luttge, A., 2007. Calcium carbonate formation and dissolution. Chem. Rev. 107 (2), 342–381.
Nehrke, G., Van Cappellen, P., 2006. Framboidal vaterite aggregates and their transformation into calcite: a morphological study. J. Cryst. Growth 287 (2), 528–530.
Nehrke, G., Poigner, H., Wilhelms-Dick, D., Brey, T., Abele, D., 2012. Coexistence of three calcium carbonate polymorphs in the shell of the Antarctic clam *Laternula elliptica*. Geochem. Geophys. Geosyst. 13 (5), Q05014.
Papadimitriou, S., et al., 2007. Biogeochemical composition of natural sea ice brines from the Weddell Sea during early austral summer. Limnol. Oceanogr. 52 (5), 1809–1823.
Papadimitriou, S., Kennedy, H., Kennedy, P., Thomas, D.N., 2013. Ikaite solubility in seawater-derived brines at 1 atm and sub-zero temperatures to 265 K. Geochim. Cosmochim. Acta 109, 241–253.
Pauly, H., 1963. Ikaite, a new mineral from Greenland. Arctic 16, 263–264.
Pelouze, M.J., 1865. Sur une combinaison nouvelle d'eau et de carbonate de chaux. C. R. Acad. Sci. 60, 429–431.
Pierrot, D., Lewis, E., Wallace, D.W.R., 2006. MS Excel program developed for CO_2 system calculations. ORNL/CDIAC-105aCarbon dioxide information analysis center, Oak Ridge National Laboratory, U.S. Department of energy, Oak Ridge, Tennessee.
Pytkowicz, R.M., Hawley, J.E., 1974. Bicarbonate and carbonate ion-pairs and a model of seawater at 25 °C. Limnol. Oceanogr. 19 (2), 223–234.
Reddy, M.M., 1977. Crystallization of calcium carbonate in the presence of trace concentrations of phosphorus-containing anions: I. Inhibition by phosphate and glycerophosphate ions at pH 8.8 and 25 °C. J. Cryst. Growth 41 (2), 287–295.
Reddy, M.M., Wang, K.K., 1980. Crystallization of calcium carbonate in the presence of metal ions: I. Inhibition by magnesium ion at pH 8.8 and 25 °C. J. Cryst. Growth 50 (2), 470–480.

Rickaby, R.E.M., et al., 2006. Potential of ikaite to record the evolution of oceanic $\delta^{18}O$. Geol. Soc. Am. 34 (6), 497–500.
Rysgaard, S., Glud, R.N., Sejr, M.K., Bendtsen, J., Christensen, P.B., 2007. Inorganic carbon transport during sea ice growth and decay: a carbon pump in polar seas. J. Geophys. Res. 112, C03016.
Rysgaard, S., et al., 2012. Ikaite crystals in melting sea ice — implications for pCO_2 and pH levels in Arctic surface waters. Cryosphere 6 (4), 901–908.
Rysgaard, S., et al., 2013. Ikaite crystal distribution in winter sea ice and implications for CO_2 system dynamics. The Cryosphere 7, 707–718.
Suess, E., et al., 1982. Calcium carbonate hexahydrate from organic-rich sediments of the Antarctic Shelf: precursors of glendonites. Science 216, 1128–1131.
Tlili, M.M., et al., 2001. Characterization of $CaCO_3$ hydrates by micro-Raman spectroscopy. J. Raman Spectrosc. 33, 10–16.
Uppström, L.R., 1974. Boron/chlorinity ratio of deep-sea water from Pacific Ocean. Deep-Sea Res. 21 (2), 161–162.
Vekilov, P.G., 2010. Nucleation. Cryst. Growth Des. 10 (12), 5007–5019.
Zhang, Y., Dawe, R.A., 2000. Influence of Mg^{2+} on the kinetics of calcite precipitation and calcite crystal morphology. Chem. Geol. 163 (1–4), 129–138.